Dissecting specific and global transcriptional regulation of bacterial gene expression

Gerosa, Luca; Kochanowski, Karl; Heinemann, Matthias; Sauer, Uwe

Published in:
Molecular Systems Biology

DOI:
10.1038/msb.2013.14

Publication date:
2013

Supplementary Material for

Dissecting specific and global transcriptional regulation of bacterial gene expression

Gerosa L, Kochanowski K, Heinemann M, Sauer U

Contents

1. Strains, growth conditions and physiology

We used a total of 16 fluorescent promoter reporter plasmids and 2 genetic backgrounds, wild type and ArgR knockout (Table S1). All promoter reporters were inserted in a *E. coli* wild type BW25113 background, in addition the 8 arginine promoters and the *epd-icd* promoter reporter plasmid were also inserted in the ArgR knockout background (Baba et al., 2006). The total number of fluorescent promoter reporter plasmid and strain combinations is 25, of which 12 are constitutive reporter strains, 11 are specifically regulated reporter strains, and 2 are the promoter less plasmids p139 inserted in ArgR knockout and wild type for background correction (see Table S1 for a detailed list of strain and plasmid combinations).

We used a total of 19 different mediums with composition listed in Table S2 to study promoter activity of constitutive promoters. Other medium compositions were used to specifically study the response of arginine pathway to arginine depletions, details are in Table S6 and Table S8. Minimal medium was prepared as follows: to 700 mL of purified and autoclaved water, 200 mL of 5x base salt solution (211 mM Na_2HPO_4, 110 mM KH_2PO_4, 42.8 mM NaCl, 56.7 mM $(NH_4)_2SO_4$, autoclaved), 10 mL of trace elements (0.63 mM $ZnSO_4$, 0.7 mM $CuCl_2$, 0.71 mM $MnSO_4$, 0.76 mM $CoCl_2$, autoclaved), 1 mL 0.1 M $CaCl_2$ solution (autoclaved), 1 mL 1 M $MgSO_4$ solution (autoclaved), 2 mL of 500x thiamine solution (1.4 mM, filter sterilized) and 0.6 mL 0.1 M $FeCl_3$ solution (filter sterilized) were added. The resulting solution was filled up to 1 L with water. In case of amino-acids in the medium, amino-acids were added to final concentrations as described in (Zaslaver et al., 2004).

We performed experiments to characterize the growth physiology and assess the reliability of the promoter reporter constructs for the combinations of strains, reporter plasmids and growth conditions used in this work. Specifically, we wanted to:

1. assure that the selected growth conditions span the entire range of *E. coli*'s physiological growth rate and evaluate eventual differences between the ArgR knockout and the wild type strain.
2. evaluate if strains carrying promoter reporters are impaired in growth rate because of the burden of expressing the GFP reporter protein.
3. compare the growth physiology obtained in the 96-well plates format to batch cultures, to allow a direct comparison of our work with traditional studies that are usually performed in aerated shakeflask batch cultures.
4. test that removal of specific regulation by scrambling transcription factor binding sites on the promoter region is effective and maintains unaltered the kinetic properties of promoters.
5. test that the dependency of constitutive promoter activity to growth rate is similar in the wild type and in the ArgR knockout strain, so that parameters inferred in a ArgR KO strain can be compared to data obtained in the wild type strain.

We report here the answers to the above questions:

1. We analyzed the steady state growth rates of our combination of strains and reporters in the 18 selected conditions. We found that wild type E. coli cells spanned rather uniformly the growth rates between 0.18 and 1.6 h^{-1} (Fig. S1a) and ArgR knockout cells spanned a slightly reduced range of growth from 0.18 h^{-1} to 1.3 h^{-1} (Fig. S1b). A comparison between growth rates in the two strains shows that in average the ArgR knockout sustains 73% of the wild type growth (Fig. S1c). The growth defect observed for the ArgR knockout strain is arguably caused by the metabolic burden of having a constantly upregulated arginine biosynthesis pathway. In Fig. S2 and Fig. S3 we show the mean growth rate with standard deviations and the logarithm of the optical density signal (OD_{600}) with standard deviations from inoculation to stationary phase for each of the 19 conditions in Table S2 for both wild type and ArgR knockout strain. Mean and standard deviation for growth rates and OD signals are calculated pulling together data from the 4 wild type strains carrying the constitutive forms of *pykF, epd, epd-icd, kbl* and of the 8 arginine promoters in the ArgR knockout strain.

2. Growth rates sustained by strains carrying different promoter reporters (with different expression levels) are extremely similar in each condition, as shown by the very low standard deviations in measurements (Fig. S1a and Fig. S1b). We concluded there is no observable burden of expressing GFP protein for any of our promoter reporters, as has also been shown previously for the same reporter library (Zaslaver et al., 2009).

3. We compared growth in shake flask and in our 96-well plate setup on two different conditions of growth: glucose minimal medium and glycerol minimal medium (Fig. S5). We found that growth was almost identical in the two different setups, demostrating that the 96 well plate setup guarantees full aeration for aerobic growth and that our result are potentially comparable with traditional studies of microbial growth.

4. We decided to compare the promoter activity of a promoter turned constitutive by the scrambling its transcription factor binding sites in the wild type strain and in a strain in which the transcription factor itself was knocked out. Of the three plasmids constructed as such, we selected the *pykF* reporter plasmid because the knockout strain of its only regulator, Cra, is still vaiable with a sufficiently fast growth in a number of conditions. For the *kbl* and *epd* promoter reporters, the knockout strains of regulators Lrp and Crp, respectively, have a substantially reduced growth rate in most conditions, and thus are not ideal for this type of test. We inserted the regulated and constitutive versions of the *pykF* promoter reporter plasmid in the Cra knockout strain (Baba et al., 2006) and measured their promoter activity during steady state growth in 8 conditions. We found that promoter activity measurements plotted against the measured growth rate are in the same range and have the same trend as the constitutive version of the *pykF* promoters in the wild type strain (Fig. S4). We concluded that the strategy of scrambling transcription factor binding is effective in removing regulation and in maintaining the kinetic properties of the promoter region.

5. We inserted the *epd-icd* constitutive promoter reporter plasmid in the ArgR knockout strains. The promoter activity measured during growth in the 18 steady state conditions follows quantitatively the trend of the same reporter plasmid in the wild type background (Fig. 1 in the main text). We concluded that the relation between promoter activity and growth rate is unaltered in the ArgR

knockout strains and thus that the kinetic parameters obtained from the ArgR knockout strain can be used to analyse promoter activity data from a wild type strain.

Plasmid	Background strain	Comments	Origin
p139	BW25113 *ΔargR* and wild type	Promoter-less plasmid strain used for background correction	This study Zaslaver et al., 2008
argA	BW25113 *ΔargR* and wild type	Native promoter	This study Zaslaver et al., 2008
argC	BW25113 *ΔargR* and wild type	Native promoter	This study Zaslaver et al., 2008
argD	BW25113 *ΔargR* and wild type	Native promoter	This study Zaslaver et al., 2008
argE	BW25113 *ΔargR* and wild type	Native promoter	This study Zaslaver et al., 2008
argF	BW25113 *ΔargR* and wild type	Native promoter	This study Zaslaver et al., 2008
argG	BW25113 *ΔargR* and wild type	Native promoter	This study Zaslaver et al., 2008
argI	BW25113 *ΔargR* and wild type	Native promoter	This study Zaslaver et al., 2008
argR	BW25113 *ΔargR* and wild type	Native promoter	This study Zaslaver et al., 2008
pykF regulated by Cra	BW25113 wild type	Native promoter	This study Zaslaver et al., 2008
pykF constitutive	BW25113 wild type	Native pykF native promoter with Cra binding site replaced by non functional equally spaced sequence. Inserted promoter sequence: TGGTTCCTGCCCCAGATCGCGCATTTCCAGCACAACTTTAC CGACAACTCTGCACATTTCTCGGTACAGTTCATCCTCTTTT GTCCGATTTCCCATTCTTTATACCTATTTATCATGCCAACTA TCAGCATATATCAATCTAACCAATTAAACAAAAATCAAACA AAATCAGACAAATAACGCGATAAATTATTTTAACTGTAGC AATTGAGCGATGATATATTTATACACCGGATGAACTTTCA CTTATCCTCACACTGACAACTTCGGCACCAGACGTTGCGC AAACAGTGAAGTTTTTGCGTAACCTTTTCCCTGGAACGTTA AATCTTTGATAACAATTTATTGTCTAACAAGTTGTATATTTT TTGAAACGCTGTTTTTGTTTTCCTTTTGGATTAATTTCAGCG TATAATGCGCGCCAATTGACT**TCAGGATATGTGGCGG**ACT TTGGACTGTAGAACTCAACGACTCAAAAACAGGCACTCAC GTTGGGCTGAGACACAAGCACACATTCCTCTGCACGCTTT TTCGATGTCACCTATCCTTAGAGCGAGGCACCACCACTTTC GTAATACCGGATTCGCTTTCCGGCAGTGCGCCCAGAAAGC AAGTTTCTCCCATCCTTCTCAACTTAAAGACTAAGACTGTC ATGAAAAAGACCAAAATTGTTTGCACCATCGGACCGAAAA C	(Kochanowski et al., 2013)
kbl regulated by Lrp	BW25113 wild type	-	This study Zaslaver et al., 2008
kbl constitutive	BW25113 wild type	Native Kbl promoter with Lrp binding site replaced by non functional equally spaced sequence. Inserted promoter sequence: TTTGCAGAAGTGTTAACGCGTTATCTCGTCGCGACCTATA AGTTTGGGTAATATGTGCTGGAATTTGCCCTGTCTGGAGA ATCGCAATGCGTGGAGAATTTTATCAGCAGTTAACCAACG ATCTGGAAACCGCACGGGCGGAAGGGTTGTTTAAAGAAG AGCGCATTATTACGTCTGCGCAGCAAG	This study

epd regulated by Cra and CRP	BW25113 wild type	Native regulated epd promoter. Inserted promoter sequence: GAGATGACTGAAGAAGGCCGGTATCACTTCACAAGCTGA CAATTTATTCCAGTTATTGTAGGGTTATTATTACGCCAGCC TGGAATAAAGCTTCCCACAAAAGGGGATAAAAGTGTGAT GTGAGTCAGATAAATGTCTTCTTCGGCTGGACAAACATTC CTTTTATTCCACGTTTCGCTTATCCTAGCTGAAGCGTTTCA GTCGATTAAATGTTCGACAATTAACCAATCAGTCGCAGTTT GCGACAGGTAAGGTTTCCCCGGACGATTTGCTGGATTACT CTGTCTGGCAAATTTGCTCAGGGAAAACCTTGCAGGAGAT CTATGACCGTACGCGTAGCGATAAATGGCTTC	This study
epd constitutive	BW25113 wild type	Native epd promoter with Cra and Crp binding sites replaced by non functional equally spaced sequences. Inserted promoter sequence: GGCTGGACAAACATTCCTTTTATTCCACGTTTCGCTTATCC T**CACGAGAGAACAACGTAA**GATTAAATGTTCGACAATTA ACCAATCAGTCGCAGTTTGCGACAGGTAAGGTTTCCCCGG ACGATTTGCTGGATTACTCTGTCTGGCAAATTTGCTCAGG GAAAACCTTGCAGGAGATCTATGACCGTACGCGTAGCGA TAAATGGCTTC	This study
epd-icd constitutive	BW25113 *ΔargR* and wild type	Native epd promoter with RNA polymerase binding site sequence replaced by RNA polymerase binding site sequence from the icd promoter. Inserted promoter sequence: TTTCATGACGGCAAACAATAGGGTAGTATTCACGAGAGAA CAACGTAAGATTAAATGTTCGACAATTAACCAATCAGTCG CAGTTTGCGACAGGTAAGGTTTCCCCGGACGATTTGCTGG ATTACTCTGTCTGGCAAATTTGCTCAGGGAAAACCTTGCA GGAGATCTATGACCGTACGCGTAGCGATAAATGGCTTC	This study

Table S1. List of the fluorescent promoter report plasmids and strains used in this study.

ID	Medium composition	Description
1	M9 + 5 g/L galactose	Galactose minimal medium (Gal)
2	M9 + 5 g/L acetate	Acetate minimal medium (Ace)
3	M9 + 5 g/L pyruvate	Pyruvate minimal medium (Pyr)
4	M9 + 5 g/L fructose	Fructose minimal medium (Fru)
5	M9 + 5 g/L succinate	Succinate minimal medium (Suc)
6	M9 + 5 g/L mannose	Mannose minimal medium (Man)
7	M9 + 5 g/L glycerol	Glycerol minimal medium (Gly)
8	M9 + 5 g/L gluconate	Gluconate minimal medium (Gnt)
9	M9 + 5 g/L glucose	Glucose minimal medium (Glc)
10	M9 + 5 g/L acetate + amino acids	Acetate min. med. with amino acids (Ace+AA)
11	M9 + 5 g/L pyruvate + amino acids	Pyruvate min. med. with amino acids (Pyr +AA)
12	M9 + 5 g/L succinate + amino acids	Succinate min. med. with amino acids (Suc +AA)
13	M9 + 5 g/L galactose + amino acids	Galactose min. med. with amino acids (Gal +AA)
14	M9 + 5 g/L mannose + amino acids	Mannose min. med. with amino acids (Man +AA)
15	M9 + 5 g/L fructose + amino acids	Fructose min. med. with amino acids (Fru +AA)
16	M9 + 5 g/L glycerol + amino acids	Glycerol min. med. with amino acids (Gly +AA)
17	M9 + 5 g/L gluconate + amino acids	Gluconate min. med. with amino acids (Gnt +AA)
18	M9 + 5 g/L glucose + amino acids	Glucose min. med. with amino acids (Glc +AA)

Table S2. List of media used to study constitutive promoter activity.

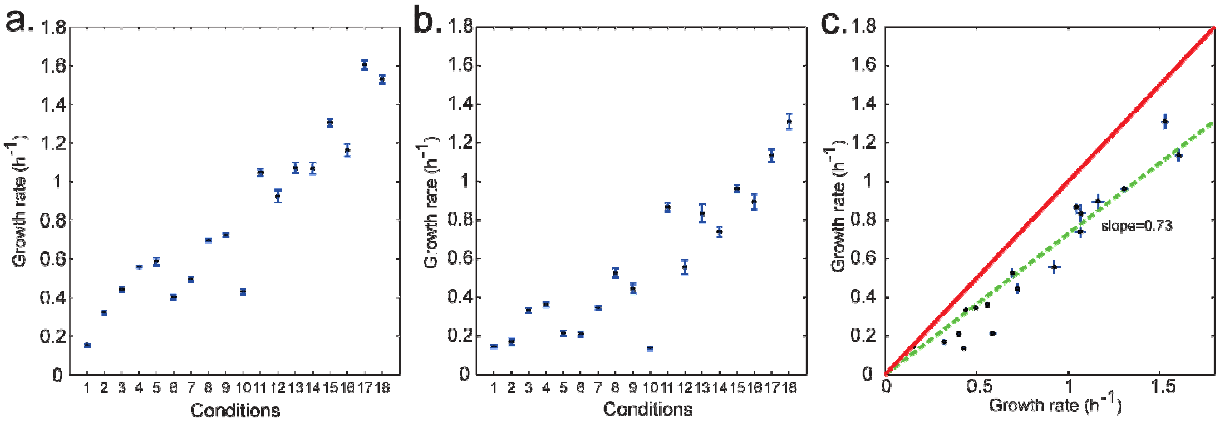

Figure S1. Steady state growth rate in 18 conditions for wild type and ArgR knockout strains. a) Growth rates in steady state in 18 conditions for the wild type strain. The shown average growth rate and standard deviation is from measurements of specifically regulated and constitutive versions of *pykF*, *kbl*, *epd*, *epd-icd* and the *p139* promoter plasmid reporters inserted in wild type strain. Conditions are numbered as in Table S2. b) Growth rate in steady state in 18 conditions for the ArgR knockout strain. The shown average growth rate and standard deviation is from measurements of the 8 arginine promoters, the *epd-icd* and the *p139* promoter plasmid reporters inserted in the ArgR knockout strain. Conditions are numbered as in Table S2. c) Comparison of steady state growth rate sustained by the wild type and the ArgR knockout strains during growth in the 18 conditions. Perfect match (red line) and match obtained from linear fit of data (dotted green line) are shown. The slope represents the average growth rate reduction of the ArgR knockout strain compared to the wild-type.

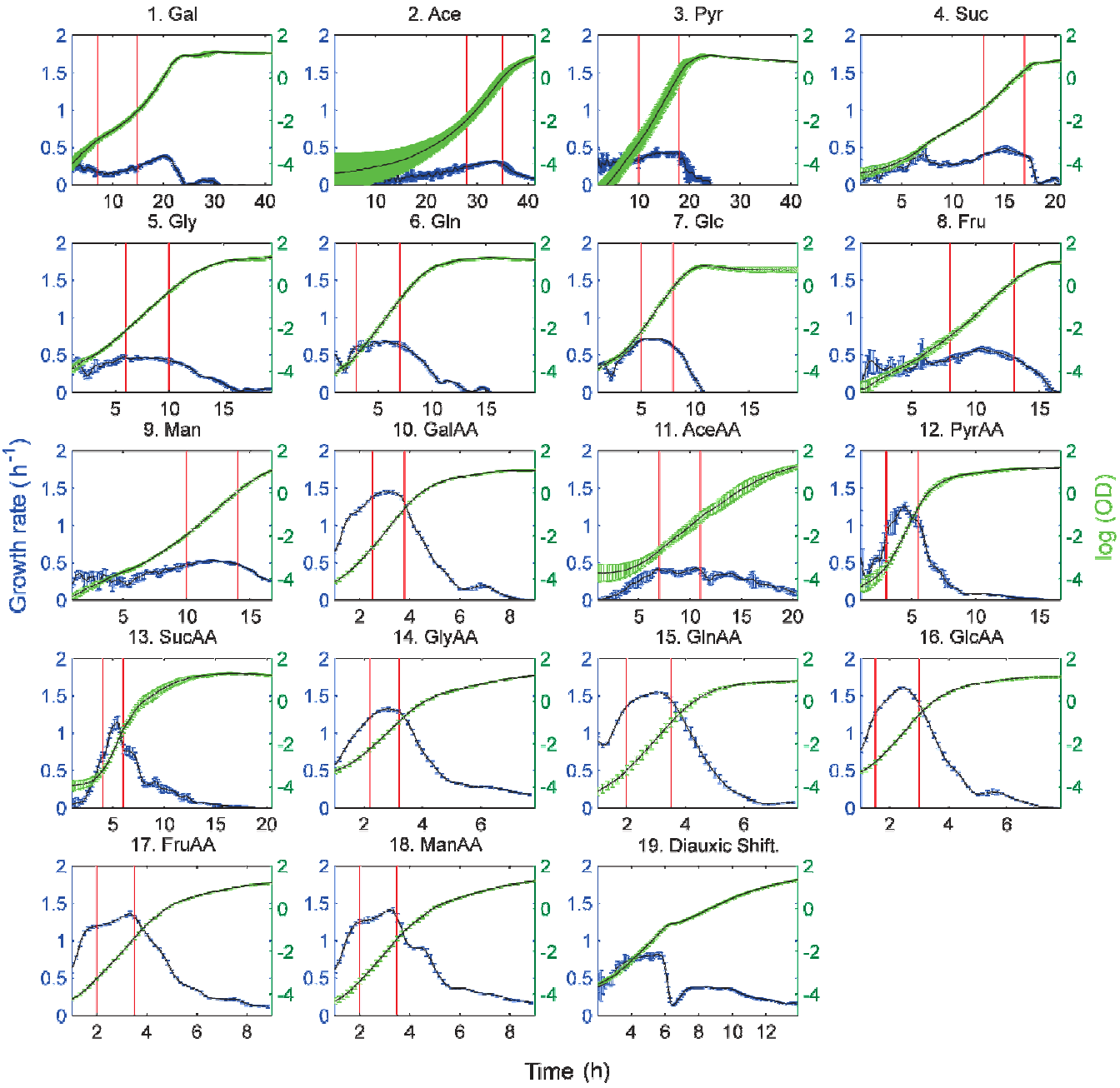

Figure S2. Time-course physiology during growth on the 19 conditions for the wild type strain. Mean growth rate (blue lines) and standard deviations (blue vertical bars), respectively, as measured across wild type strains during growth in the 19 conditions as described in Table S2. Mean logarithm of OD_{600} signal (green lines) and standard deviations (green vertical bars), respectively, as measured across wild type strains during growth in the 19 conditions as described in Table S2. The phase of growth that we identified as steady state growth is indicated between red continuous lines.

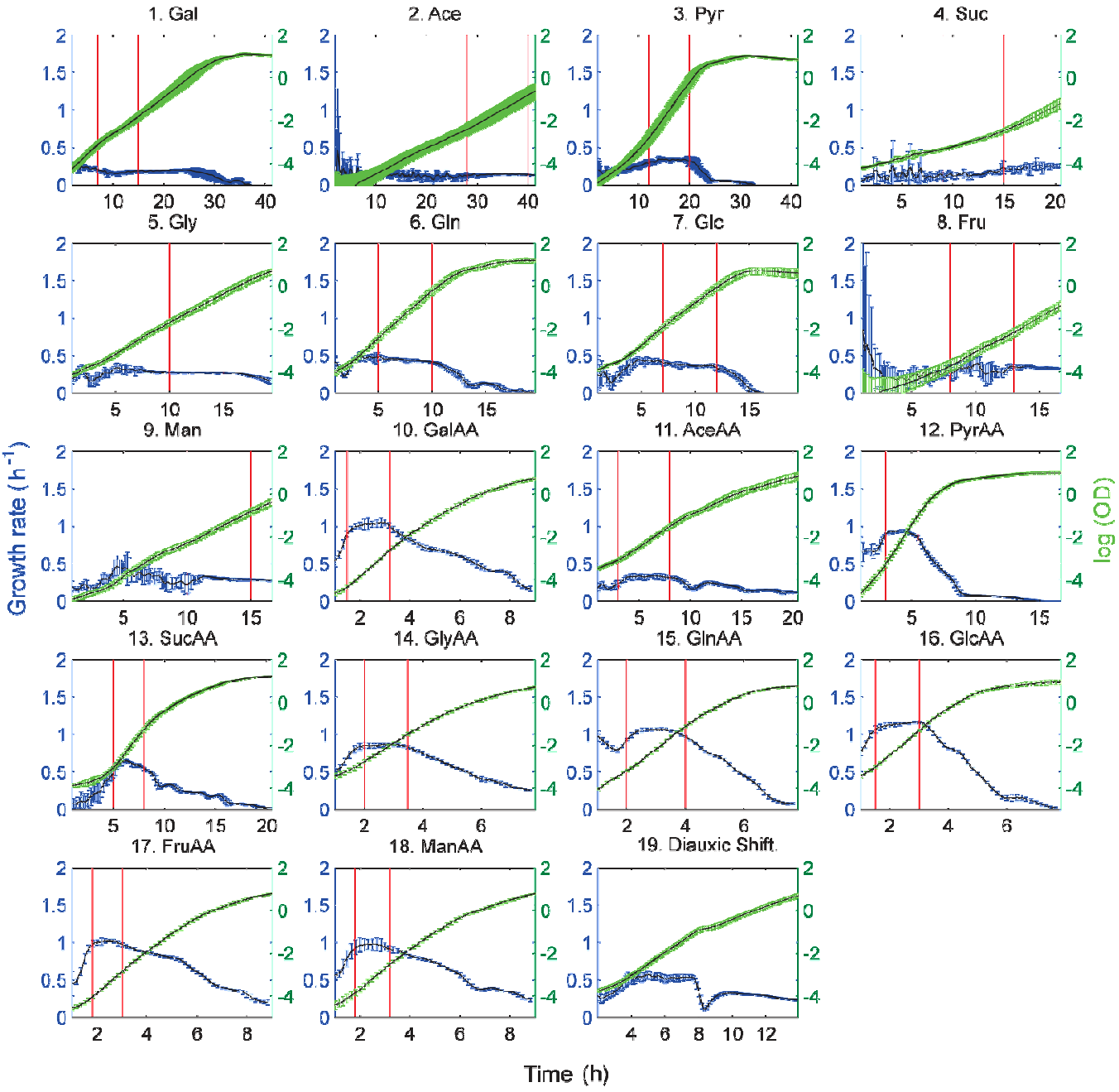

Figure S3. Time-course physiology during growth on the 19 conditions for the ArgR knockout strain. Mean growth rate (blue lines) and standard deviations (blue vertical bars), respectively, as measured across ArgR knockout strains during growth in the 19 conditions as described in Table S2. Mean logarithm of OD_{600} signal (green lines) and standard deviations (green vertical bars), respectively, as measured across wild type strains during growth in the 19 conditions as described in Table S2. The phase of growth that we identified as steady state growth is indicated between red continuous lines.

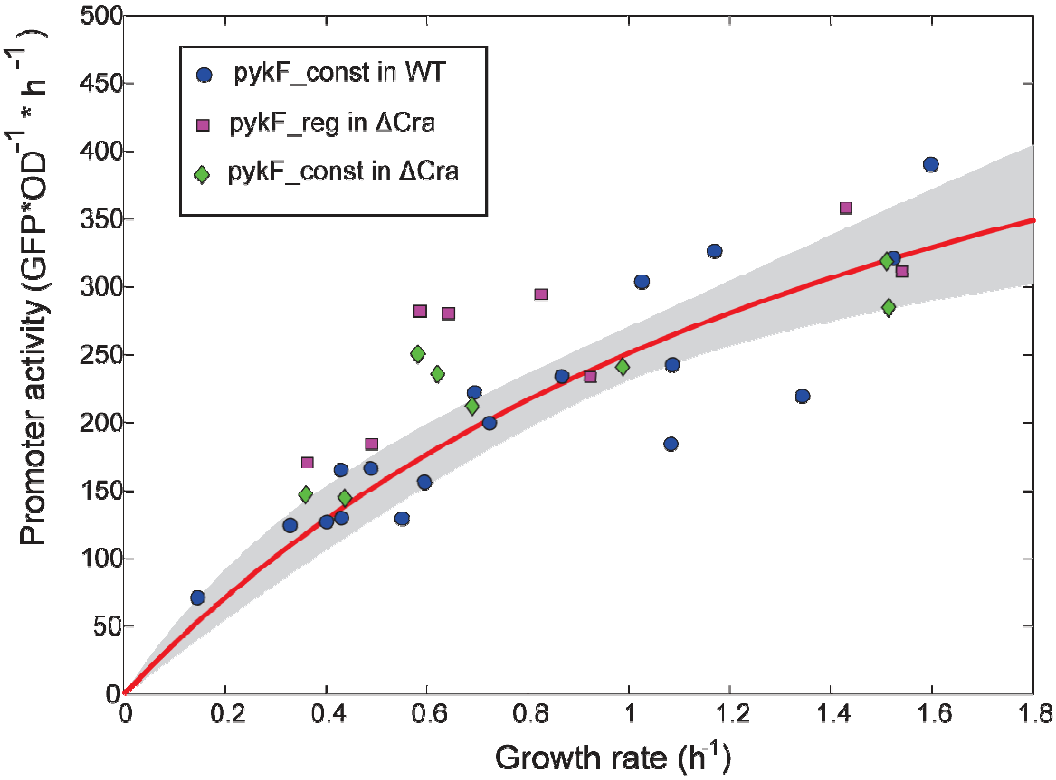

Figure S4. Promoter activity as function of growth rate for the constitutive and regulated *pykF* promoter reporter in wild type and Cra knockout strains. Blue dots show promoter activity and growth rate data for the constitutive version of the *pykF* promoter reporter (pykF_const) in the wild type strain measured in the 18 steady state conditions (data shown also in Fig. 1 main text). Magenta squares and green diamonds show the regulated (pykF_reg) and constitutive version of the pykF promoter reporter inserted in a Cra knockout strain, respectively. The 8 conditions of growth for strains in the Cra knockout are: succinate, glycerol, gluconate, glucose minimal medium and succinate, glycerol, gluconate and glucose minimal medium plus amino acids. The Michaelis Menten fitting (red line) and upper and lower bounds (shaded gray area) are shown, as described in the main text and shown in Fig. 1 in the main text.

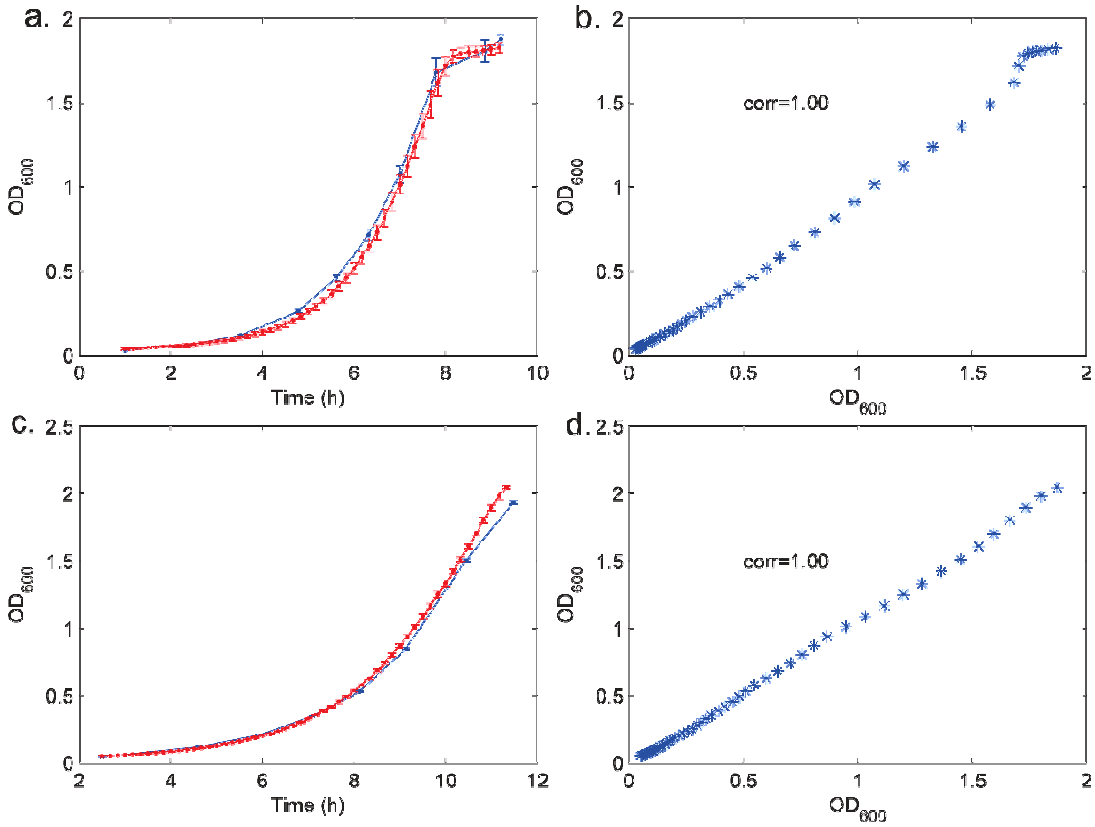

Figure S5. Comparison of growth physiology in shake flask and in the 96 well plate. a) Growth on glucose minimal medium (2 g/L glucose) of wild type strain in aerobic shake flask (blue line) and 96 well plate (red line). Average and standard deviation of the time-course OD_{600} signal are from 3 and 4 replicates for shake flask and 96-well plate, respectively. b. Comparison between shake flask and 96 well plate OD_{600} signal. The correlation is calculated by Pearson correlation. c) Growth on glycerol minimal medium (2 g/L glycerol) of wild type strain in aerobic shake flask (blue line) and 96 well plate (red line). Average and standard deviation of the time-course OD_{600} signal are from 3 and 4 replicates for shake flask and 96-well plate, respectively. d) Comparison between shake flask and 96 well plate OD_{600} signal.

2. Model for specific and global regulation of bacterial gene expression

Here we derive mathematically and provide the quantitative information to develop Eq.1 and Eq.2 in the main text. We describe the expression of GFP from reporter plasmids using two time-dependent ordinary differential equations, one for mRNA and the other for GFP concentration in a single cell as in (Klumpp, Zhang, & Hwa, 2009):

SE1 $$\frac{d[m]}{dt} = \alpha_m \cdot [g] - (\beta_m + \mu) \cdot [m]$$

SE2 $$\frac{d[gfp]}{dt} = \alpha_p \cdot [m] - (\beta_p + \mu) \cdot [gfp]$$

The first equation describes intracellular mRNA concentration (m) as function of the plasmid copy number in the cell (g), the transcription rate sustained by a single promoter region (α_m) and the mRNA degradation rate (β_m). The second equation shows that the GFP protein concentration is a function of the mRNA amount, the translation rate (α_p) and the GFP degradation rate (β_p). Both mRNA and protein concentrations are additionally subjected to dilution by growth (μ). Square brackets represent intracellular concentrations, so that $[c]=c/v$ for an intracellular amount c and the cell volume v. Following the derivation in steady state in (Klumpp et al., 2009) we can write GFP concentration as:

SE3 $$[gfp] = (\alpha_m \cdot \alpha_p \cdot g) / (\beta_m \cdot \mu \cdot v)$$

where we used information (see Table S3) that the *GFPmut2* fluorescent protein is highly stable and negligible compared to dilution ($\beta_p << \mu$) and that mRNA degradation is much faster than dilution ($\beta_m >> \mu$) to simplify the relationship. We did not include in the model any delay due to GFP maturation because the GFP variant used in this study has an extremely fast maturation time (~5-7 mins) (Zaslaver et al., 2006). Promoter activity, our measure of gene expression, is calculated from the total population fluorescence (GFP) and Optical Density (OD). Since in exponential growth GFP is produced with an exponential rate equal to the growth rate and OD has been reported to be proportional to the total cell volume (Table S3), we can derive an equivalence between promoter activity and the gene expression model:

SE4 $$pa = \frac{dGFP}{dt \cdot OD} = \mu \cdot \frac{GFP}{OD} = \mu \cdot [gfp] = (\alpha_m \cdot \alpha_p \cdot g) / (\beta_m \cdot v)$$

Given that the gene expression cascade parameters α_m, α_p, g, β_m and v in the above equivalence are potentially varying depending on growth conditions, additional information is necessary to determine which parameters primarily govern promoter activity. Importantly, in exponential growth the quantitative trend of most of the parameters within the gene expression model has been shown to be either constant or a function of the growth rate, irrespective of the growth medium (Klumpp et al., 2009)(Bremer & Dennis, n.d.). In Table S3 we summarized the known growth rate-dependent trends of each gene expression parameter. We additionally determined that pMS201 plasmid copy number and gene copy number on the chromosome have a rather constant ration of 5 to 1 across steady state (Fig. S6a) and dynamic growth (Fig. S6b) by comparing activities of a plasmid borne and a chromosomally inserted promoter. Further, we used the Cooper and Helmstetter (Cooper & Helmstetter, 1968) relation to calculate the growth rate-dependent copy number of the

chromosomally inserted gene and divided it by the growth rate-dependent cell volume of *E. coli* cells (Kubitschek, 1974) to finally determine that plasmid concentration is constant across growth rates both in steady and dynamic growth (Fig. S6c). We could conclude that in steady state promoter activity is proportional to the only growth rate-dependent parameter, the transcription rate α_m, with proportionality term given by the constant translation rate α_p, mRNA degradation β_m and plasmid copy number [g]. Such proportionality term is identical across constructs if there are only minor differences in translation rate and mRNA stability across different reporters. The mRNA sequences transcribed from promoter reporters used in this study have possibly some differences in the leading mRNA sequence, which comes from the native promoter region (Zaslaver et al., 2006), but an identically strong ribosomal binding site in front of the GFP coding region to equalize the affinity for the ribosome. If such construction effectively delivers identical mRNA properties across reporters, then promoter activity is a proxy to transcription rate that is also quantitatively comparable across promoters. If instead mRNA properties are somehow different across constructs, then the Vmax term incorporates also translational effects and comparison across promoters is additionally influenced by the rate of mRNA degradation or translation. Nevertheless, promoter activity remains a proportional proxy to transcription rate, just with a possibly different proportionality across reporters. We used the results presented in SE4 to derive Eq.1 in the main text. The bases to derive Eq. 2 are given in full in the main text.

Parameter(s)	Quantitative information	Reference
α_m (transcription rate)	α_m is positive non-linear function of growth rate .	(Klumpp et al., 2009)(Liang et al., 1999)
β_m (GFP degradation rate)	β_m is constant across growth rates and dominates over dilution.	(Klumpp et al., 2009)
α_p (translation rate)	α_p is constant across steady state growth rates.	(Klumpp et al., 2009)
β_p (GFP degradation rate)	β_p is low and negligible compared to dilution.	(Zaslaver et al., 2006)
OD (optical density)	OD, optical density is proportional to total cell population volume.	(Klumpp et al., 2009)
g ∝ v (plasmid copy number, single cell volume)	[g] is constant across steady state and dynamic growth. Obtained dividing cell volume and plasmid copy number, which have the same growth rate-dependency.	(Kubitschek, 1974),(Cooper & Helmstetter, 1968) and this work, Fig. S6c.

Table S3. Quantitative parameters of bacterial gene expression and pMS201 reporter plasmid across growth rates.

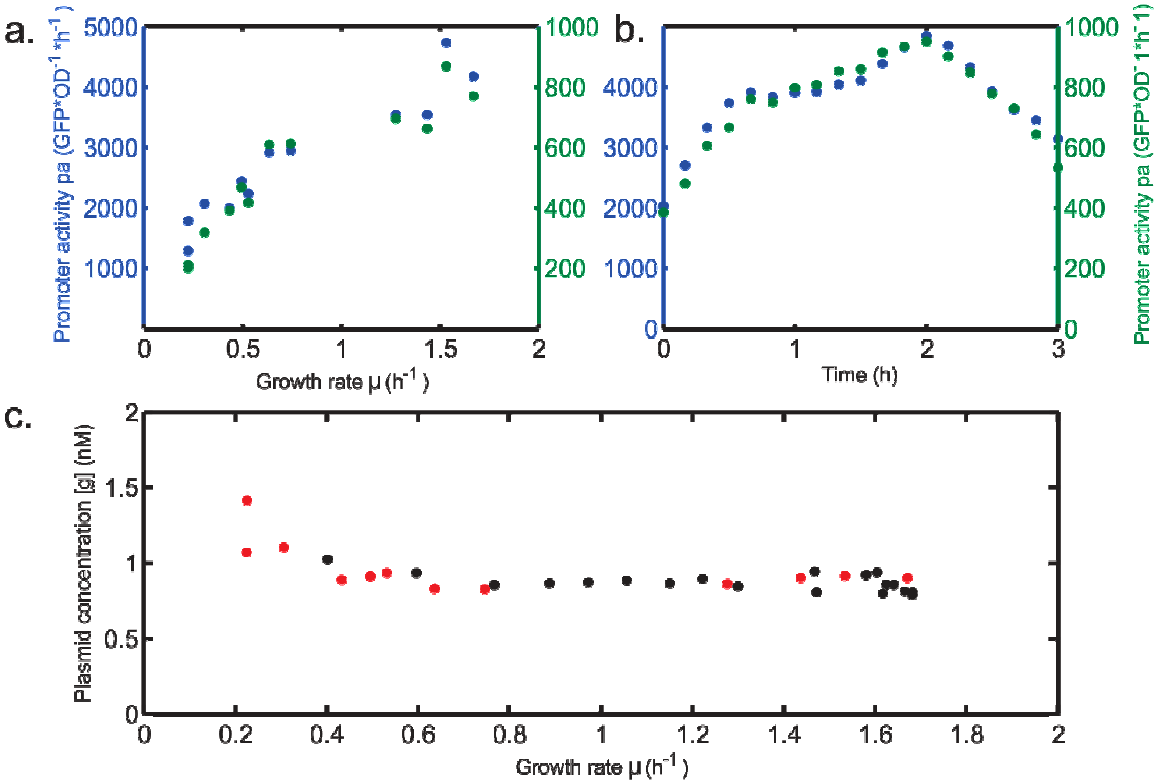

Figure S6. Plasmid concentration (pMS201) as function of growth rate across steady state and dynamic growth. a) Promoter activity of the hisL promoter expressing GFP from plasmid (blue dots) or from the chromosome (green dots) at different steady state growth rates (notice different scales on y-axis). Growth conditions are, in order of increasing growth rate: galactose, acetate, pyruvate, glycerol, succinate, fructose, gluconate, glucose minimal medium andglycerol, galactose, gluconate and glucose minimal medium with amino acids. b) Promoter activity of the hisL promoter expressing from plasmid (blue dots) and from the chromosome (green dots) in a time-course growth in glucose minimal medium supplemented with amino acids. c) Plasmid intracellular concentrations at different growth rates calculated by dividing plasmid copy number per cell by the growth-rate dependent cellular volume as give in (Kubitschek, 1974). Plasmid copy number per cell as a function of growth rate was calculated by multiplying the hisL chromosomal copy number per cell obtained by the Cooper and Helmstetter relation (Cooper & Helmstetter, 1968) by the ratio between promoter activities of plasmid borne and chromosomally inserted hisL (red dots are steady state data, black dots are time-course data). The ratio between plasmid-borne and chromosomal promoter activity was 5 to 1 across most of the sampled growth rates.

3. Fitting of constitutive parameters on steady state data

Estimation of V_{max} and K_m parameters from steady state promoter activity and growth rate was done by least square minimization. First, we tested the performance of the Michaelis-Menten rate law in describing steady state constitutive promoter activity by calculating the percentage error between measurement and fit data points. We found an average error of 16% across the promoter and conditions, without substantial difference across promoters or conditions (Figure S5).

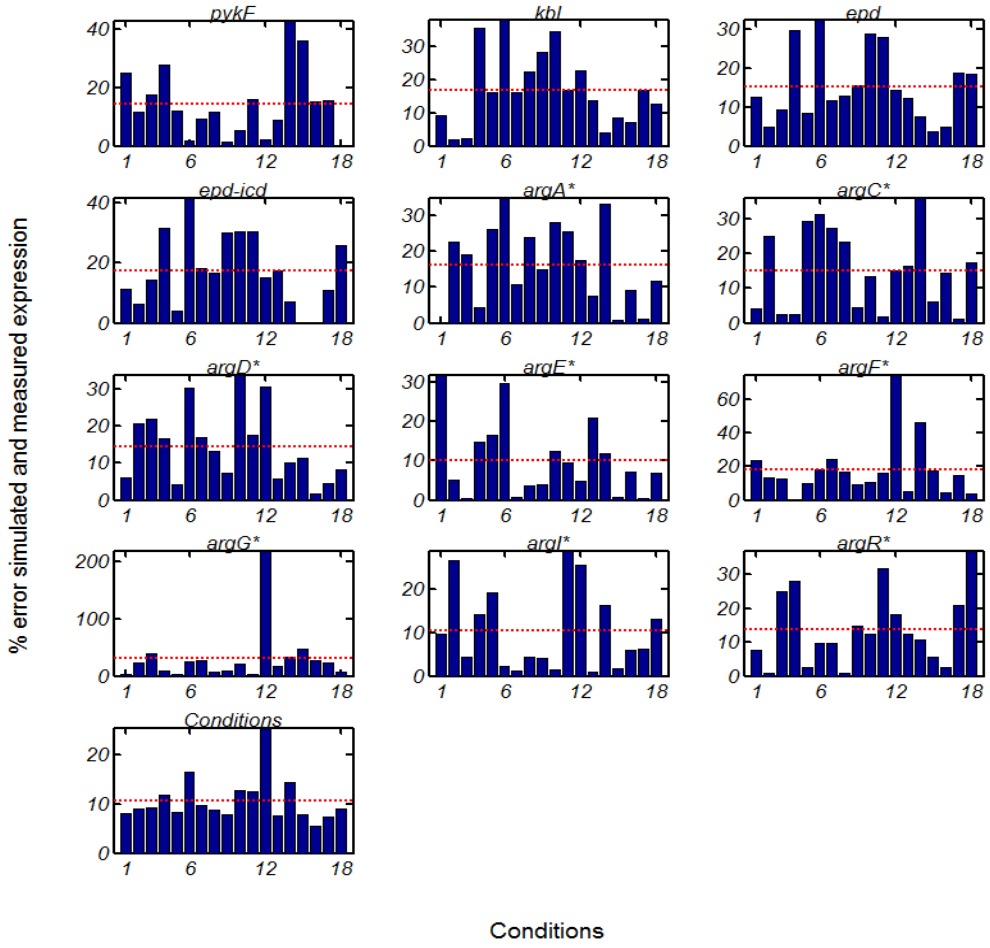

Figure S7. Percentage error between experimental and model fit promoter activity for constitutive genes. For each promoter (first 12 plots) and for each condition (last plot), the percentage error between experimental promoter activity and simulated promoter activity according to the Michaelis-Menten fitting is shown. Dotted red lines show the average across the x-axis. On the x-axis, conditions are numbered as in Table S2.

We further tested V_{max} and K_m robustness to perturbations in the measured data points to assure that measurement errors were not decisive in the fitting. We performed two different type of stress on data: the first progressively removing data-points and the second progressively adding noise to the data. We inferred the average V_{max} and K_m parameter estimation as function of number of data points removed (Fig. S8) or as function of the uniform random noise added and calculated the percentile deviation from the optimal V_{max} and K_m parameter set (Fig. S9). Results show V_{max} and K_m estimates to

be rather robust to up to 3 points removal (Fig. S8) and within 20% of random uniform error addition (Fig. S9). Thus, we regard our V_{max} and K_m estimates as robust upon reasonable deviations in the measured data.

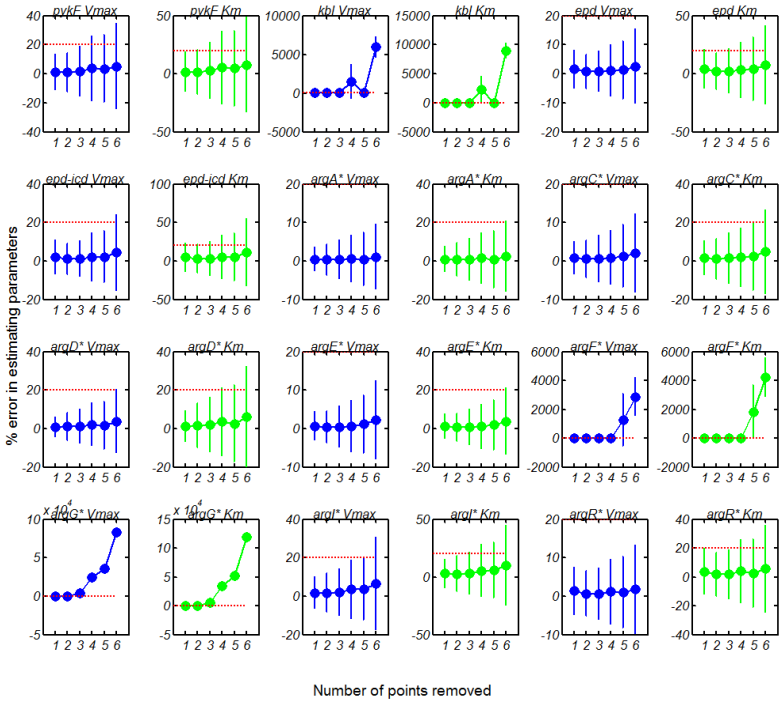

Figure S8. Robustness of constitutive parameter estimation to data point elimination. Percentage error in estimating V_{max} and K_m from data as function of number points removed from original data.

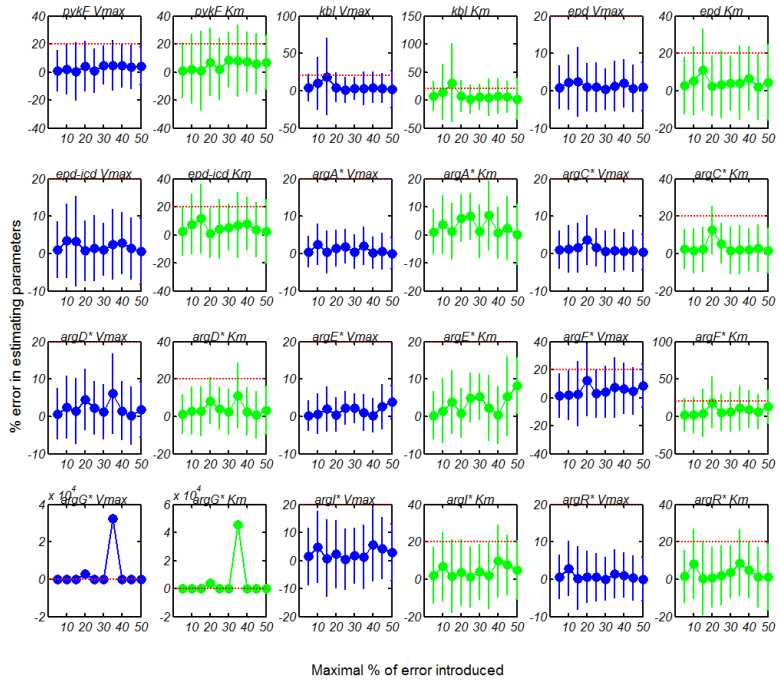

Figure S9. Robustness of constitutive parameter estimation to data addition of random uniform error. Percentage error in estimating V_{max} and K_m from data as function of percentage of added noise to all data points simultaneously.

To evaluated the uniqueness of V_{max} and K_m parameter estimation we evaluated alternative of V_{max} and K_m pair values that fit data within a suboptimal sum squared error. We generated a grid of values pairs spanning from 0 to 15000 ($GFP*OD^{-1}*h^{-1}$) for V_{max} and from 0 to 5 (h^{-1}) for K_m. We considered parameter pairs that fit the data within a sum squared error of 5%, 10% and 20% from the optimal. We found that lower and upper bound for V_{max} and K_m parameters calculated as such were often large and scaled with the absolute value of parameters (Fig. S10) but the area spanned by the alternative fitting curves was rather contained near the optimal curve (Fig. 1 main text). This can be understood as the promoter activity data being in many cases not fully saturated in the sampled growth rate range, so that an increase in V_{max} can be compensate by an increase in K_m to fit the non-linear trend across growth rate. Indeed, we found that distribution of V_{max} and K_m pairs in the parameter space that fit the data within the 5%, 10% and 20% of the optimal sum squared error are related by a proportionality term. Importantly, the parameter space of suboptimal V_{max} and K_m pairs is well defined and individual for each promoter, so that difference across K_m and across V_{max} parameters is relevant.

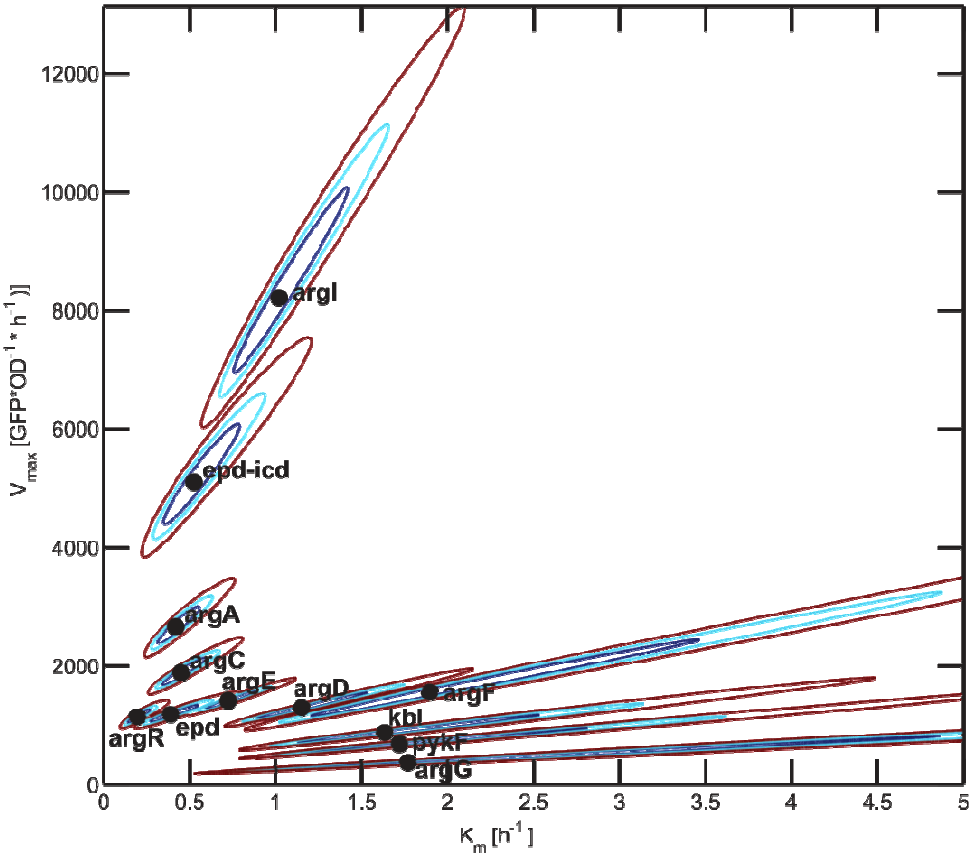

Figure S10. Distribution of V_{max} and K_m constitutive parameters and their suboptimal parameter space. Distribution of V_{max} and K_m parameter estimates for the 12 constitutive promoters by least-square criteria (black dots). Contour plot of the suboptimal parameter space within 5% (blue line), 10% (cyan line) and 20% (brown line) error from the optimal sum squared error.

Next we tested if the Michalis-Menten law is a good fit specifically for constitutive promoters or in general would be a good fit also for specifically regulated promoter. We calculated the Pearson linear correlation coefficients and relative p-value of the steady state promoter activity and growth rate data that where linearized using the Lineweaver-Burk reciprocal relation:

SE5 $$\frac{1}{pa} = \frac{K_m}{V_{max}} \cdot \frac{1}{\mu} + \frac{1}{V_{max}}$$

We obtained a statistical significance value for the fitting of a Michaelis-Menten rate law type on constitutive and specifically regulated promoter activity (Fig. S11). In addition to the 12 constitutive promoters and the 11 specifically regulated versions, we measured four additional specifically regulated promoters that were supposed to be strongly regulated across the measured 18 conditions, metA, sera, pckA and sdhC. The Michaelis-Menten relationship between growth rate and promoter activity was statistically significant (p-value<0.01) for all constitutive and only for two regulated promoters. Because for these two promoters, *pykF* and *kbl*, the constitutive version had nevertheless a much higher statistical significance than the regulated version, presumably the promoters are only weakly or growth-dependently regulated, so that the constitutive backbone of promoter activity on top of which regulation is operating is partially observed in the statistical test.

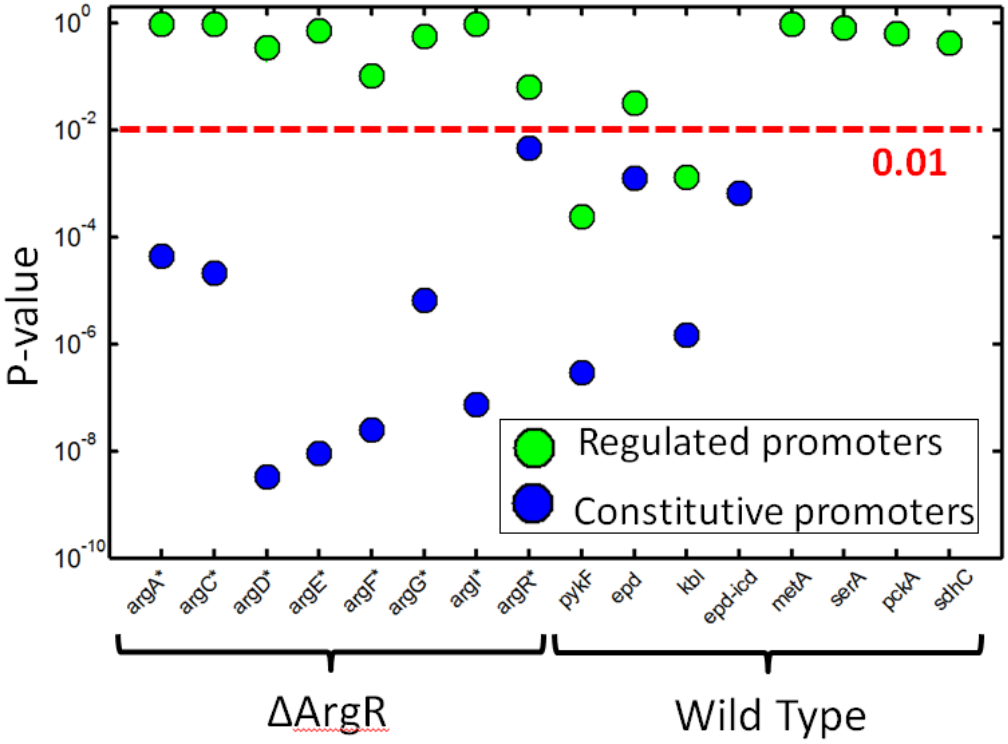

Figure S11. Statistical significance of Michaelis-Menten rate law fit for constitutive and specifically regulated promoter. On the x-axis the name of promoters for which steady state promoter activity and growth rate was measured across the 18 steady state conditions previously described, on the y-axis the statistical significance expressed as p-value of Pearson correlation against their linearized relationship using Lineweaver-Burk reciprocal. As a hybrid promoter, epd-icd has no regulated counterpart. The last four promoters metA, serA, pckA and sdhC have no constructed constitutive counterpart but were included to show that known strongly regulated promoters have indeed low statistical significance.

4. Predicting constitutive promoter activity during dynamic changes in growth rate

We used Eq. 2 in the main text to predict constitutive promoter activity of the 12 constitutive promoter reporter strains during dynamic growth in 19 different conditions. The OD and GFP signals of the cultures were measured online from inoculation till arrest of growth as described in the Material and Methods section. OD measurements were converted into the instantaneous growth

rate μ by calculating numerically the slope between each two points of the log OD signal. Together with V_{max} and K_m parameters as reported in the Table 1 of the main text, growth rate was used to predict constitutive promoter activity using Eq.2 in the main text. Measured and predicted promoter activity (shown in Fig. S12) were compared by calculating two statistical tests: Pearson correlation and the Coefficient of Determination R^2.

We calculated the two indicators in two different ways: first, for the aggregate of the data that were concatenated across all promoters and conditions, and found that the overall predictive power was very accurate with a Pearson correlation of 0.85 and p-value < 10^{-9} , an overall R^2=0.73. Then, we performed the same tests for each of the promoters in each individual condition, with results summarized in Table S4 for Pearson Correlation and in Table S5 for the Coefficient of Determination R^2.

Corr	epd	pykF	kbl	epd-icd	argA	argC	argD	argE	argF	argG	argI	argR	**Mean**
Gal	0.93	0.90	0.90	0.92	0.88	0.86	0.81	0.80	0.73	0.64	0.90	0.85	0.84
Ace	0.87	0.18	0.72	0.91	0.06	0.18	-0.03	-0.02	0.27	0.30	-0.17	-0.01	0.27
Pyr	0.94	0.75	0.75	0.94	0.90	0.96	0.94	0.95	0.76	0.37	0.95	0.94	0.85
Fru	0.80	0.81	0.82	0.69	-0.14	0.17	0.18	0.68	0.27	0.12	0.13	0.41	0.41
Suc	0.81	0.75	0.87	0.87	0.73	0.54	0.00	0.67	0.20	0.24	0.73	0.69	0.59
Man	0.84	0.62	0.76	0.90	0.57	0.73	0.58	0.78	0.43	-0.04	0.74	0.38	0.61
Gly	0.89	0.86	0.82	0.81	0.44	0.56	0.10	0.41	-0.18	0.56	-0.07	0.06	0.44
Gln	0.95	0.95	0.98	0.97	0.89	0.83	0.76	0.90	0.70	-0.33	0.96	0.83	0.78
Glc	0.93	0.95	0.95	0.94	0.82	0.79	0.91	0.91	0.81	0.76	0.94	0.87	0.88
AceAA	0.87	0.74	0.88	0.89	0.54	-0.45	0.09	0.28	-0.26	-0.06	0.32	0.71	0.38
PyrAA	0.91	0.88	0.93	0.94	0.94	0.96	0.90	0.87	0.86	0.27	0.95	0.92	0.86
SucAA	0.87	0.85	0.94	0.91	0.90	0.78	0.90	0.78	0.64	0.35	0.85	0.87	0.80
GalAA	0.96	0.74	0.96	0.97	0.87	0.77	0.97	0.96	0.83	0.25	0.75	0.49	0.79
ManAA	0.77	0.34	0.96	0.93	0.68	-0.03	0.72	0.80	0.58	0.02	0.68	0.58	0.59
FruAA	0.87	0.60	0.99	0.92	0.82	0.55	0.69	0.78	0.65	0.19	0.74	0.73	0.71
GlyAA	0.98	0.41	0.91	0.98	0.91	0.37	0.90	0.90	0.62	0.13	0.50	0.90	0.71
GlnAA	0.92	0.88	0.95	0.97	0.90	0.85	0.74	0.72	0.59	0.11	0.92	0.91	0.79
GlcAA	0.97	0.77	0.97	0.99	0.98	0.96	0.89	0.92	0.78	0.59	0.98	0.97	0.90
Shift	0.93	0.69	0.70	0.91	0.91	0.85	0.86	0.77	0.75	0.74	0.90	0.54	0.79
Mean	0.90	0.72	0.88	0.91	0.72	0.59	0.63	0.73	0.53	0.28	0.67	0.67	0.68

Table S4. Correlation coefficient between measured and simulated promoter activity in dynamic growth.

R^2	epd	pykF	kbl	epd-icd	argA	argC	argD	argE	argF	argG	argI	argR	**Mean**
Gal	0.85	0.32	0.75	0.84	0.74	0.71	0.63	0.54	0.30	0.24	0.69	0.72	0.61
Ace	0.74	-2.01	0.27	0.65	-2.45	-5.48	-0.15	-0.42	0.01	-0.10	-1.89	-0.88	-0.98
Pyr	0.88	0.47	0.56	0.87	0.72	0.89	0.74	0.88	0.48	0.09	0.89	0.83	0.69
Fru	0.47	0.48	0.26	0.27	-0.35	-0.06	-0.04	-0.05	-0.29	-2.48	-0.15	0.16	-0.15
Suc	0.53	-0.47	0.69	0.64	0.42	-0.01	-1.03	0.38	-1.37	-0.14	-0.47	0.29	-0.04
Man	0.46	-0.34	0.47	0.42	-0.19	0.11	0.06	0.22	-1.30	-0.83	-0.15	0.07	-0.08
Gly	0.79	0.25	0.65	0.58	-0.98	-1.42	-0.92	0.04	-0.66	-2.29	-1.65	-0.19	-0.48
Gln	0.90	0.59	0.95	0.94	0.70	0.64	0.56	0.30	0.46	-4.06	0.78	0.66	0.29
Glc	0.85	0.82	0.88	0.85	0.56	0.58	0.78	0.81	0.23	0.40	0.70	0.75	0.68
AceAA	0.05	0.43	0.12	0.36	0.06	-1.43	-0.11	0.03	-0.28	-0.04	-0.25	-0.15	-0.10
PyrAA	0.71	0.74	0.82	0.72	0.77	0.83	0.79	0.73	0.68	0.03	0.71	0.71	0.69
SucAA	0.72	0.58	0.85	0.80	0.78	0.48	0.76	0.57	0.23	-0.62	0.70	0.51	0.53
GalAA	0.83	0.32	0.84	0.84	0.27	-0.28	0.23	0.73	0.06	-0.10	-0.68	-0.32	0.23
ManAA	0.57	-0.08	0.89	0.80	0.45	-0.40	0.50	0.52	0.24	-0.39	-0.16	0.20	0.26
FruAA	0.71	0.19	0.93	0.80	0.49	0.16	-0.19	0.09	0.39	-1.78	0.32	-0.02	0.18
GlyAA	0.80	-0.19	0.71	0.81	0.34	-0.87	0.33	0.66	-0.35	-0.81	-1.07	0.04	0.03
GlnAA	0.81	0.49	0.83	0.89	0.67	0.53	0.53	0.27	0.22	-0.07	0.41	0.80	0.53
GlcAA	0.92	0.44	0.93	0.95	0.86	0.82	0.70	0.68	0.45	0.23	0.77	0.86	0.72
Shift	0.70	0.15	0.38	0.55	0.32	0.53	0.39	0.53	0.12	0.21	0.77	-0.05	0.38
Mean	0.70	0.17	0.67	0.71	0.22	-0.19	0.24	0.40	-0.02	-0.66	0.01	0.26	0.21

Table S5. Coefficient of determination R^2 between measured and simulated promoter activity in dynamic growth.

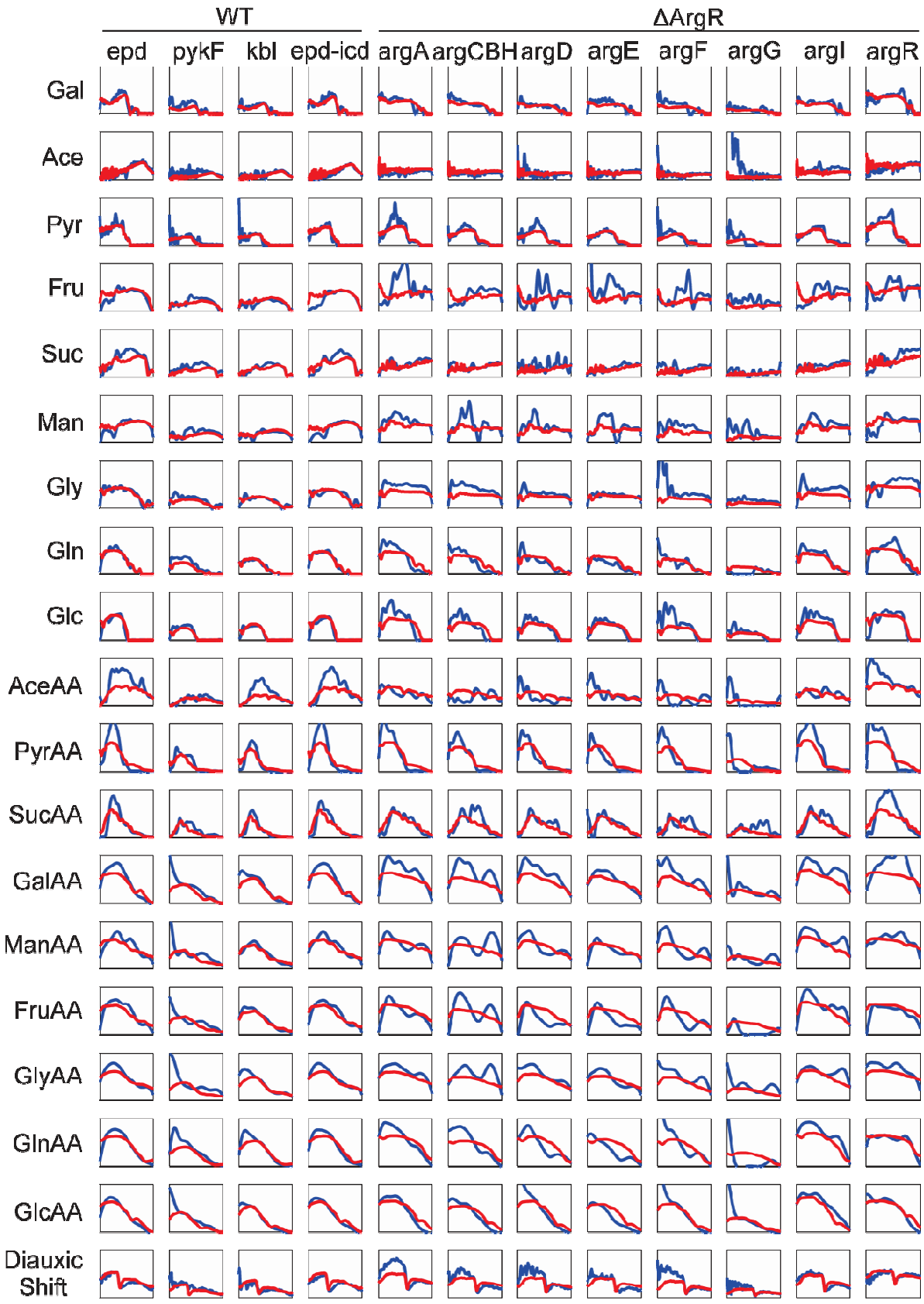

Figure S12. Measured (blue lines) and simulated (red lines) promoter activity for 12 constitutive promoters in 19 condition of growth with transient changes in growth rate. The first four promoters are in wild-type strain, the last 8 in the ArgR knockout strain. The time scale (x-axis) is identical in each condition (rows) and the promoter activity scale (y-axis) is identical for each promoter (columns).

5. Fitting specific transcriptional regulation parameters of the arginine repressor circuit

We obtained the estimate for the ArgR repressor affinity to the 8 arginine promoters by fitting steady state data using Eq. 3 developed in the main text. We used the measurements of promoter activity pa_x^i and the growth rate μ^i as a proxy to free RNAPσ^{70} concentration. We used data for the 8 promoters argx with $x \in$ {A, CBH, D, E, F, G, I, R} and for the 18 steady state conditions i=1,..,18 to infer the ArgR transcription factor activity in each condition $ArgR^{*i}$ and the ArgR dissociation constant for each promoter K_r^x by minimizing the squared percentage error across all conditions and promoters:

SE6
$$\min_{K_r^x,\, ArgR_i^*} \sum_{x \in X} \sum_{i \in I} \left(\left(pa_x^i - pa_{argx}^i\left(\mu^i, V_{max}^x, K_m^x, ArgR_i^*, K_r^x\right)\right) / pa_x^i \right)^2$$

Estimate values for K_r^x are in Table 1 of main text and Fig. S13a, for $ArgR_i^*$ in Fig. S13c. We noticed that enzymatic promoters were substantially repressed even when biosynthesis was required, to estimate the extent we calculated the average time the ArgR repressor is bound to the promoter by using the thermodynamic interpretation of Eq.3 in the main text. Under the assumption of mutual exclusion between RNA polymerase and ArgR repressor, the percentage of time is calculated as:

SE7
$$\%\_time\_ArgR\_bound_{argx}^i = \frac{ArgR^{*i}/K_r^x}{1 + \mu^i/K_m^x + ArgR^*/K_r^x}$$

In Fig. S13b are shown the percentage of time bound by ArgR. Confirming our observations, enzymatic promoters are often bound for more than 80% of the time even in conditions of arginine biosynthesis. The promoter of the repressor ArgR is instead bound only around 40% of the time in biosynthesis as a result of its 10 fold weaker affinity to the repressor. The precision of the fitting giving the inferred parameters is shown for each promoter in Fig. S14.

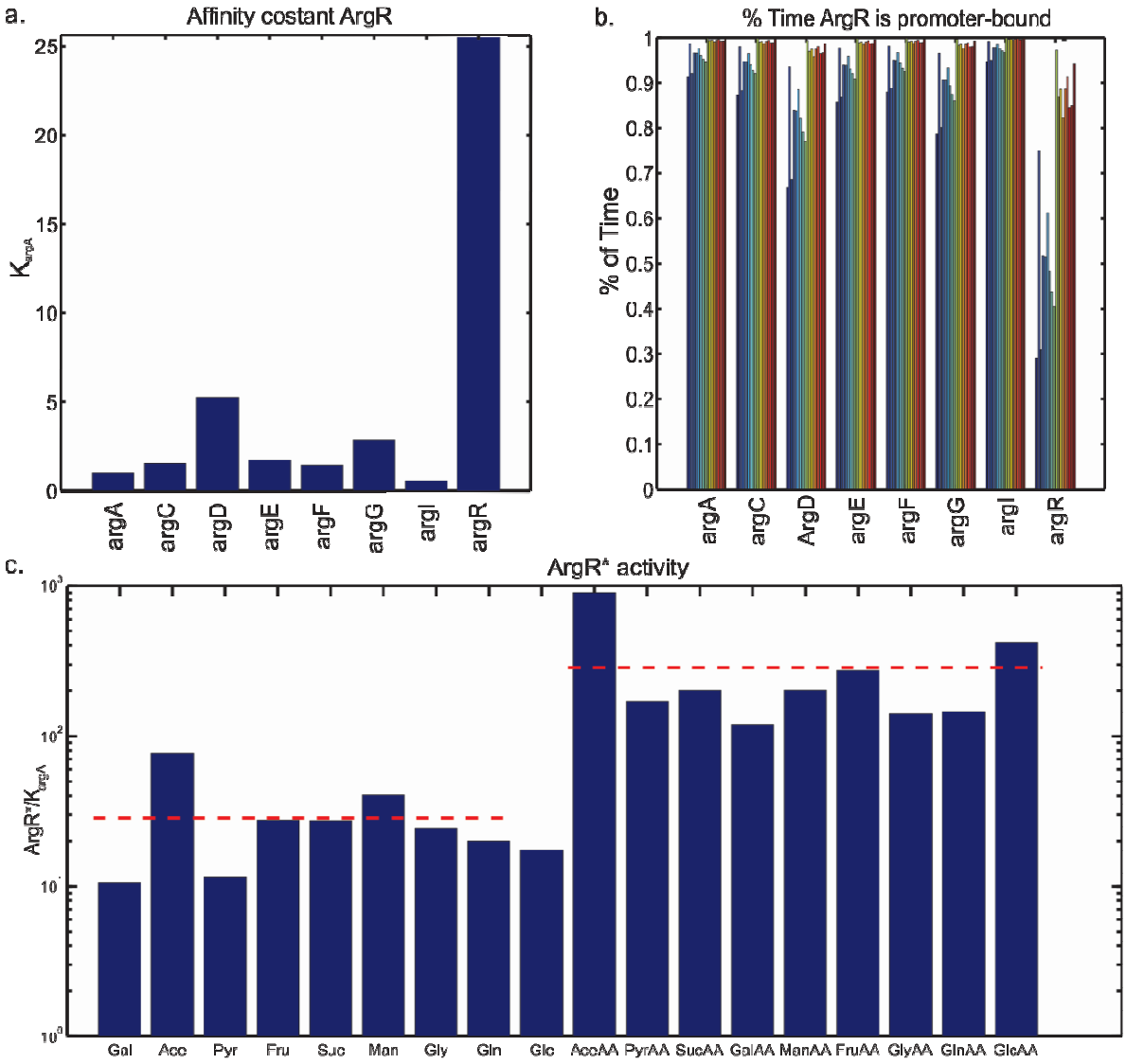

Figure S13. Fitting of specific transcriptional regulation parameter from steady state data. a) Estimate parameter values of the ArgR dissociation constants for each promoter, values are given in Table 1 of main text. b) Percentage of time the ArgR repressor is promoter-bound as calculated from the thermodynamic interpretation of promoter activity for each of the 18 steady state conditions. Order of conditions is as in plot c. c) ArgR activity as inferred from the 18 steady state conditions. The two red bars show the average activity across the 9 conditions without external supplemented arginine and the 9 conditions with external supplemented arginine, respectively.

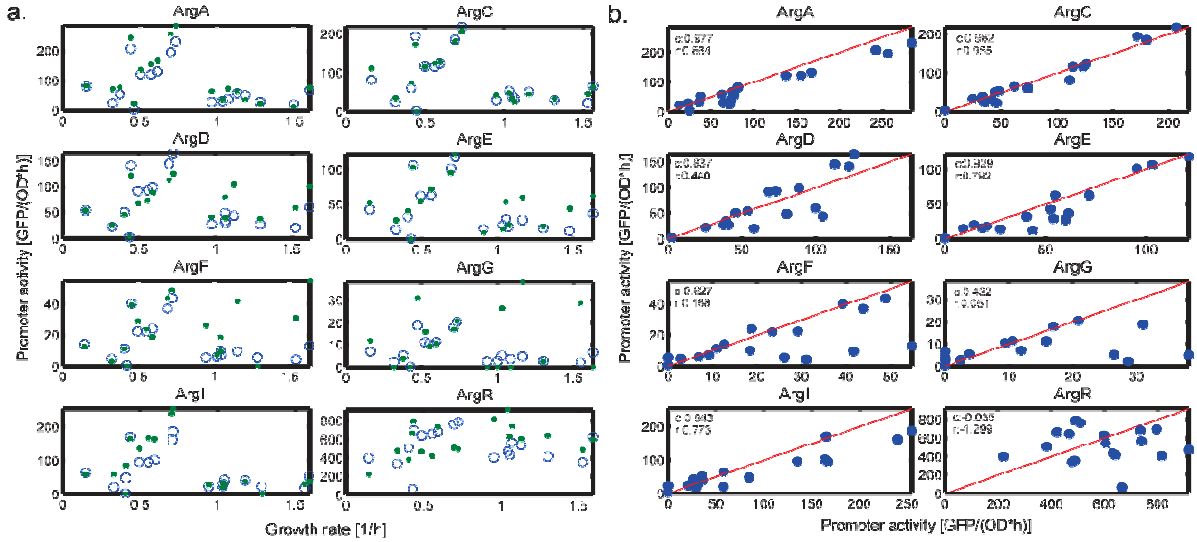

Figure S14. Reconstruction of steady state promoter activity for specifically regulated arginine promoters using fit parameters. a) Measurements (green dots) and corresponding reconstructions (blue open circles) of promoter activity for the 8 arginine promoters in the 18 steady state conditions using the inferred ArgR activity and Kr dissociation constant. b) Quantitative comparison between measurements (x-axis) and reconstructions (y-axis) of promoter activity (blue dots) for the 8 argine promoters. Person correlation (p) and coefficient of determination (r) are shown for each promoter in the corresponding insert.

6. Specific and global regulation of arginine pathway during an arginine shift

We measured the promoter activity of the 8 reporter strains for the regulated arginine promoters during 3 experiments in which growth rate was kept rather constant (Fig. S15a) and an arginine depletion shift was induced. The three medium compositions are described in Table S6.

We calculated promoter capacity, the constitutive promoter activity set by the growth rate-dependent global regulation, using Eq. 3 in the main text for each of the 8 arginine promoters in each of the three exponential growth conditions with arginine depletion, as explained in the main text. In Fig. S15b we show the comparison between regulated and constitutive promoter activity for each promoter and condition and in Fig. S16 we quantified to which extent promoter capacity is used in each of the three phases of growth: growth on externally supplemented arginine (E), transition from external supplement to biosynthesis (T), and biosynthesis (B) .

ID	Medium composition	Description
20	M9 + 5 g/L galactose + 0.09 mM arginine	Galactose minimal medium (Gal) and arginine
21	M9 + 5 g/L glucose + 0.045 mM arginine	Glucose minimal medium (Glc) and arginine
22	M9 + 5 g/L glucose + all amino acids but arginine to high concentration + 0.045 mM arginine	Glucose minimal medium (Glc) with all amino acids except arginine added to the high

Table S6. List of media used to study regulation upon arginine depletion in steady state growth.

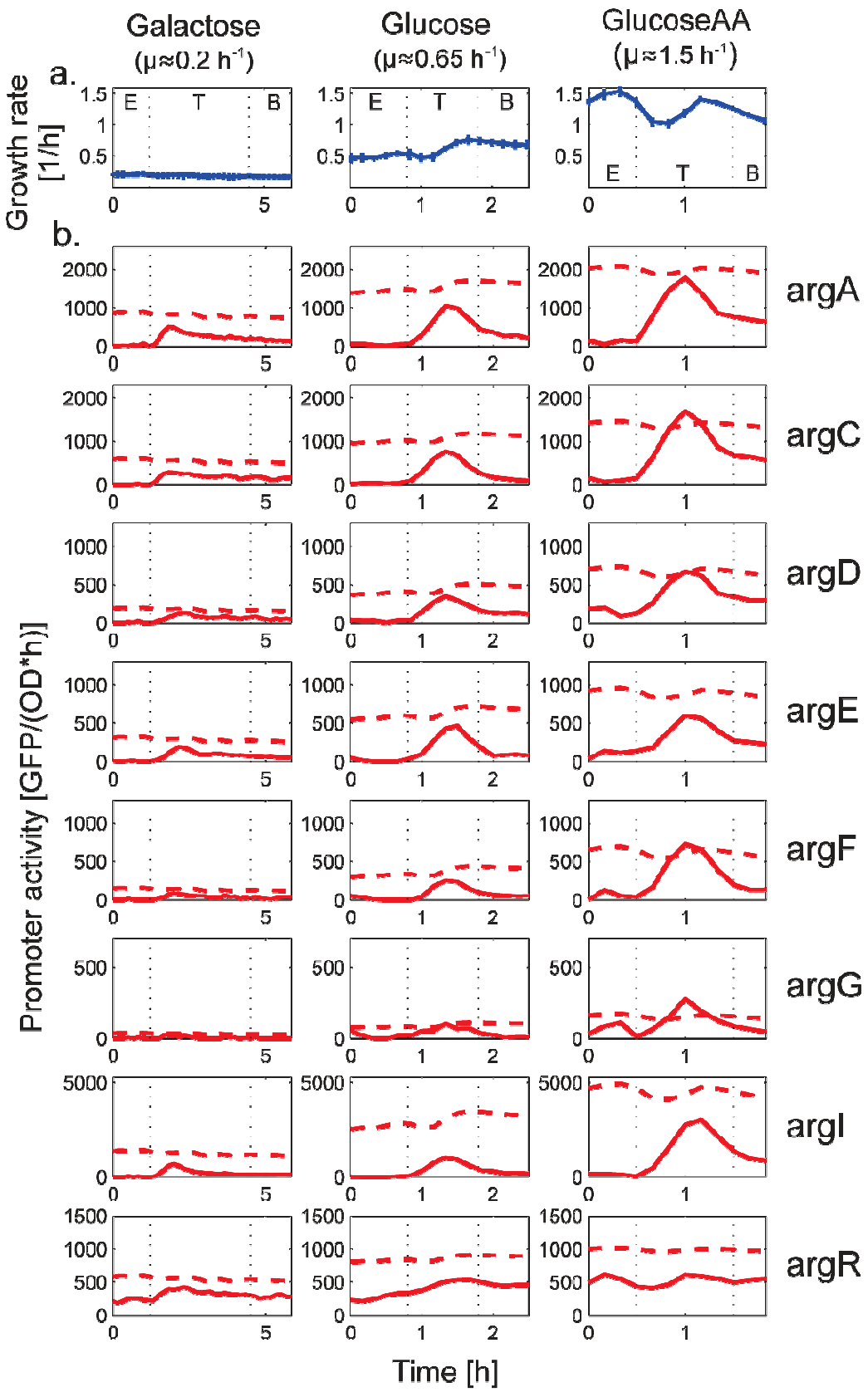

Figure S15. Growth and promoter activity in response to depletion of externally supplemented arginine. a) Growth rate average (blue horizontal line) and standard deviation (vertical blue lines) of the 8 arginine promoter reporter strains for cells growing in each of the three arginine shifts. The three phases of growth on externally supplemented arginine (E), transition from external supplement to biosynthesis (T), and biosynthesis (B) are highlighted. b) Activities of the eight arginine promoters

in response to depletion of externally supplemented arginine during exponential batch growth in three conditions. The red continuous line represents the measured regulated promoter activity and the red dotted line represents the simulated growth rate dependent promoter capacity.

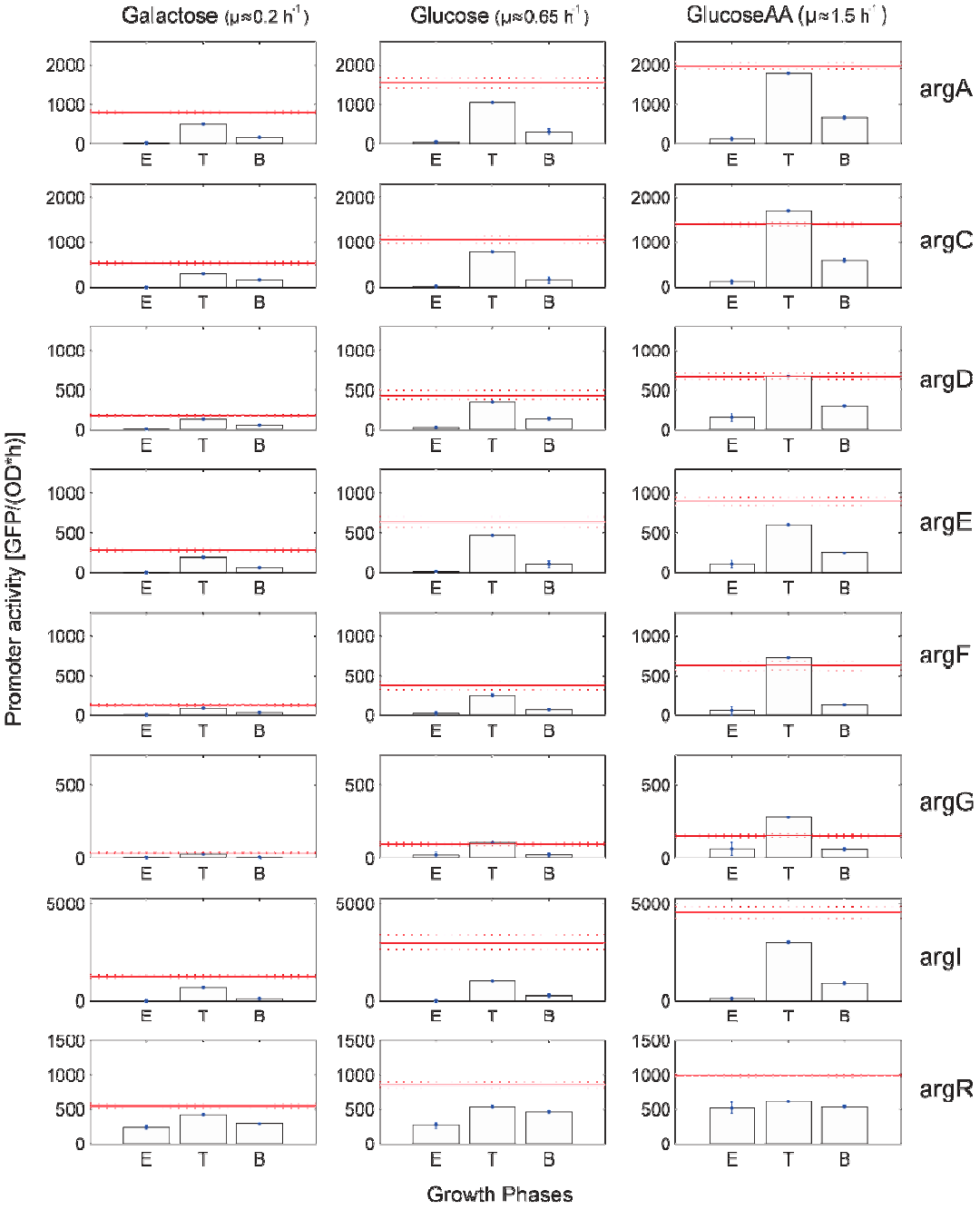

Figure S16. Quantification of promoter activity regulation in the three phases of the arginine shift. For each of the three condition of growth (columns) and for each arginine promoters (rows), we quantified regulated promoter activity with respect to the three phases of growth: externally supplemented arginine (E), transition from external supplement to biosynthesis (T), biosynthesis (B). For phases E and B, the promoter activity value is the average (with standard deviation indicated by the blue vertical lines) across time, for the phase T, is the maximal value reached by the promoter activity burst. The average constitutive promoter activity (red continuous line) and its standard deviation (red dotted line) during the time-course is shown.

7. Experiments and simulations of the arginine pathway under simultaneous global and specific regulation

To obtain a comprehensive, pathway-level understanding of regulation in the arginine pathway we developed an Ordinary Differential Equation (ODE) model of the arginine pathway including specific and global regulation and the metabolic pathway. The interactions within the pathway and regulation are shown in the main text in Fig. 3a together with the ODE model equation in Fig. 3b. The specific and global regulatory parameters (V_{max},K_m,K_r) are available as inferred from the steady state data (see Table 1 in the main text). To infer the six missing parameters in the ODE model, we decided to fit the ODE model against the ArgR activity obtained from the three dynamic arginine depletion experiments during exponential growth (Fig. 4 in the main text). First, we inferred the ArgR activity for each of the three dynamic arginine depletion experiments using a minimization of the sum squared percentage error across the 8 arginine promoters:

SE9
$$\min_{ArgR_t^*} \sum_{x\in X} \sum_{t\in T} \left(\left(pa_x^t - pa_{argx}^t\left(\mu^i, V_{max}^x, K_m^x, ArgR_t^*, K_r^x\right)\right)/pa_x^t \right)^2$$

Where $x\in${A, CBH, D, E, F, G, I, R} are the arginine promoter, T=1,..,n are the time points of measurement across the dynamics, and the free RNAP is approximated using the measured growth rate μ^i across time points. The three inferred ArgR activities underlying the repressor circuit response during the shift at different rate of exponential growth are shown in the main text (Fig. 4c).

Having obtained the three ArgR activity signals underlying the three arginine shifts, to estimate the six parameters k_{cat}, K_{deg}, K_{arg}, r_b, *n* and k_p we minimized the sum squared error of the ODE model in reconstructing the ArgR activity. We did not use the whole time-course data, but only the ArgR activity starting from the onset of promoter activity upregulation (indicated in the main text by the line dividing the E and Tgrowth phases in Fig. 4). To find the best parameter set, we ran a minimization function with different random initial values for the 6 unknown parameters and for the arginine concentration for 500 times and took the parameter set that showed the minimal percentage sum squared error across the three experiments. As starting values, we assumed no presence of ArgA enzyme in the fully repressed initial time point (ArgA(t=0)=0), we set the initial amount of ArgR as the average of the measured expression profile at the time of upregulation onset (ArgR(t=0)=800). The best fitting was obtained with the set k_{cat}=0.32, K_{deg}=0.64, K_{arg}=1.3, r_b=68, *n*=2.6 and k_p=148, and initial conditions ArgR=800, ArgA=0, arg=71. In Table S7, we provide a list of the parameters obtained from the best fit, with a description of their biological interpretation and the units in which they are expressed. The model was used to simulate the overall regulation and metabolic activity of the arginine pathway subjected to the double perturbations in growth rate and arginine availability. Simulation was performed starting from each of 12 onset times as indicated in the main text in Fig. 5. Initial conditions were set to ArgR=800, ArgA=0, arg=71 and simulation was run with as only input the measured growth rate in the diauxic shift (without any arginine in the medium) as proxy for the free RNAP and dilution. The resulting simulated promoter activity in the 12 different shifts is shown in Fig. 5 in the main text for *argA* and in Fig. S17 for the other arginine promoters. The promoter activity before upshift was calculated assuming constant abundance of arginine concentration, equal to the estimated for the initial point of upregulation (arg=71). The underlying simulations of ArgA concentration, ArgR concentration, arginine concentration and ArgR* activity can be seen in Fig. S18. The sensitivity to initial values was tested and the model was found to be robust to a large range of values for ArgR and arginine (arg) initial values (Fig. S19).

The resulting promoter activity simulations were compared with the time-course measurements for the 8 arginine regulated promoter reporters grown in 12 different media that caused arginine to run out at different points during a diauxic shift (see Table S8).

Identifier	Type	Unit	Description	Estimate Value/ Initial Condition
k_{cat}	Parameter	a.u. $\cdot h^{-1} \cdot GFP^{-1}.OD$	enzyme turnover for ArgA	0.32
k_{deg}	Parameter	h^{-1}	degradation rate for ArgA	0.64
r_b	Parameter	a.u.	biomass requirement	68
n	Parameter	-	arginine cooperativity in binding ArgR	2.6
k_p	Parameter	a.u	arginine affinity to ArgR	148
k_{arg}	Parameter	h^{-1}	arginine degradation rate	1.3
ArgR	Variable	GDP/OD	concentration of ArgR	800
ArgA	Variable	GFP/OD	concentration of ArgA	0
arg	Variable	a.u.	concentration of arginine	71
μ	Input	h^{-1}	growth rate	measurement

Table S7. Parameters, variables and inputs in the ODE model for the arginine biosynthesis pathway.

ID	Medium composition	Description
23	M9 + 0.5 g/L glucose + 5 g/L succinate + 0.03 mM arginine	Diauxic shift with arginine shift
24	M9 + 0.5 g/L glucose + 5 g/L succinate + 0.045 mM arginine	Diauxic shift with arginine shift
25	M9 + 0.5 g/L glucose + 5 g/L succinate + 0.06 mM arginine	Diauxic shift with arginine shift
26	M9 + 0.5 g/L glucose + 5 g/L succinate + 0.075 mM arginine	Diauxic shift with arginine shift
27	M9 + 0.5 g/L glucose + 5 g/L succinate + 0.0825 mM arginine	Diauxic shift with arginine shift
28	M9 + 0.5 g/L glucose + 5 g/L succinate + 0.09 mM arginine	Diauxic shift with arginine shift
29	M9 + 0.5 g/L glucose + 5 g/L succinate + 0.105 mM arginine	Diauxic shift with arginine shift
30	M9 + 0.5 g/L glucose + 5 g/L succinate + 0.12 mM arginine	Diauxic shift with arginine shift
31	M9 + 0.5 g/L glucose + 5 g/L succinate + 0.135 mM arginine	Diauxic shift with arginine shift
32	M9 + 0.5 g/L glucose + 5 g/L succinate + 0.15 mM arginine	Diauxic shift with arginine shift
33	M9 + 0.5 g/L glucose + 5 g/L succinate + 0.225 mM arginine	Diauxic shift with arginine shift
34	M9 + 0.5 g/L glucose + 5 g/L succinate + 0.3 mM arginine	Diauxic shift with arginine shift

Table S8. List of media used to induce simultaneous specific and global regulation of the arginine biosynthesis pathway.

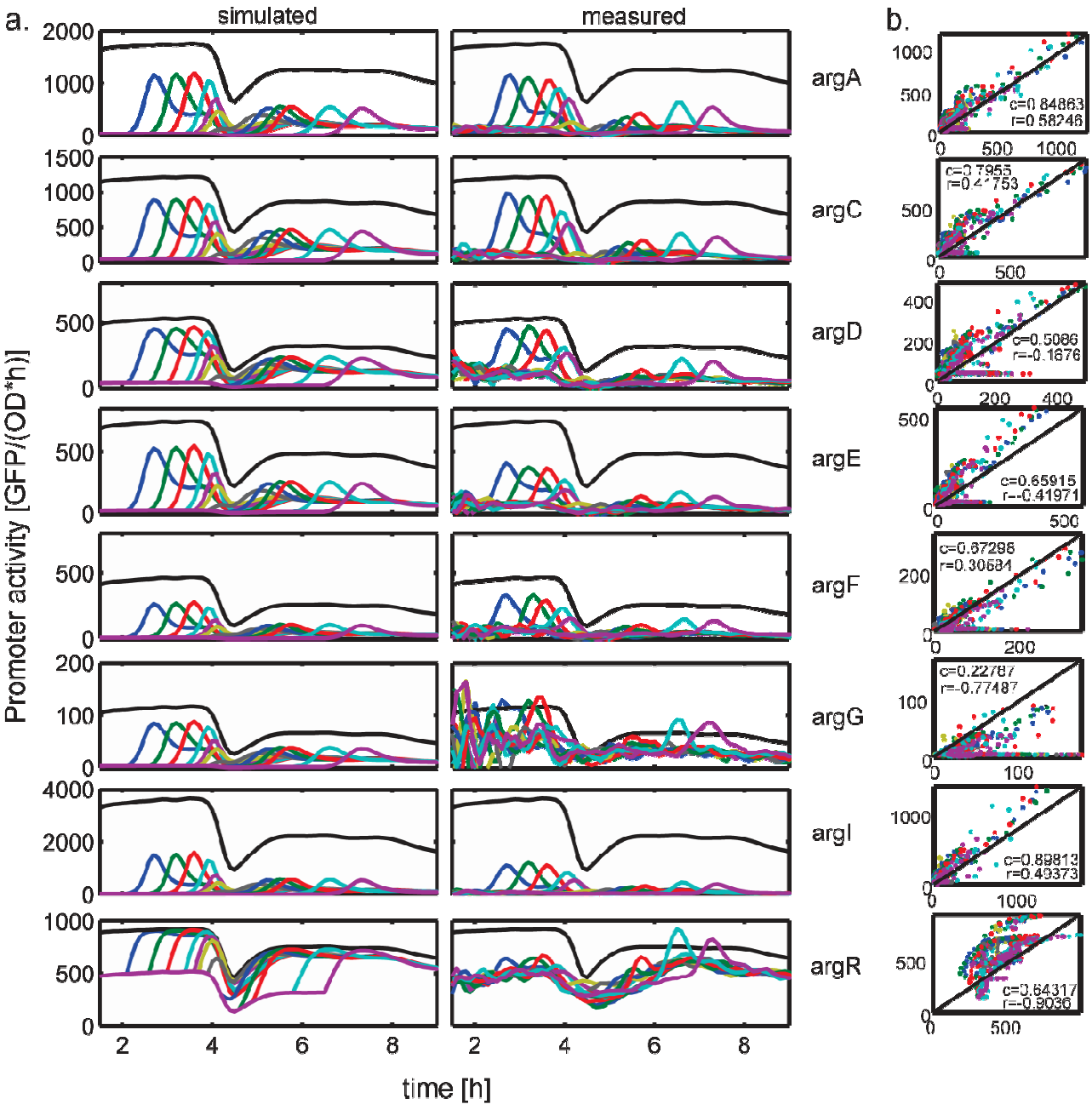

Figure S17. Measured and simulated promoter activity under simultaneous dynamic perturbations in specific and global regulation. In 12 independent experiments a different arginine concentration was supplemented and cells depleted it at different time points during the course of growth in a diauxic shifts from glucose to succinate. a) The promoter activity for each arginine promoter as measured and as simulated by the ODE model is shown. The corresponding constitutive promoter activity is shown as a black line in both plots. b) Quantitative comparison between measured and simulated promoter activity, Pearson correlation (c) and Coefficient of Determination (r) are given.

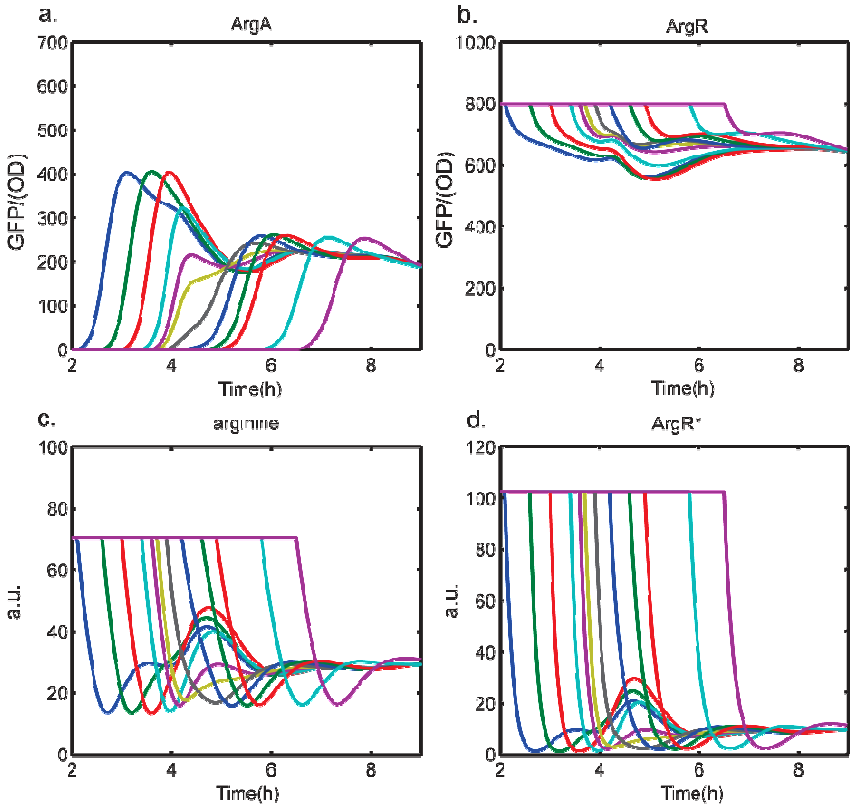

Figure S18. Simulated component abundance in simultaneous of dynamic perturbations in both specific and global regulation. a) ArgA concentration, b) ArgR concentration, c) arginine concentration and d) amount of active, arginine-not-bound ArgR (ArgR*).

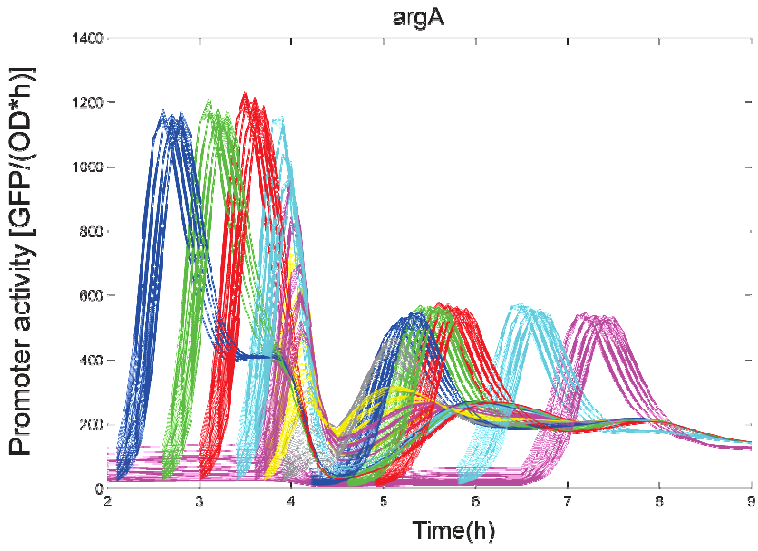

Figure S19. Sensitivity of simualtions to initial values for ArgR and arginine concentrations. Promoter activity for the argA promoter as simulated in the 12 double perturbation experiments using the ODE model under a combination of different ArgR and arginine (arg) initial values. Tested initial values are: ArgR= [600,700,800,900,1000] and arg=[50,60,71,80,90].

References

Baba, T., Ara, T., Hasegawa, M., Takai, Y., Okumura, Y., Baba, M., Datsenko, K. a, et al. (2006). Construction of Escherichia coli K-12 in-frame, single-gene knockout mutants: the Keio collection. *Molecular systems biology*, *2*, 2006.0008. doi:10.1038/msb4100050

Bremer, H., & Dennis, P. P. (n.d.). Modulation of Chemical Composition and Other Parameters of the Cell by Growth Rate. *Escherichia coli and Salmonella: Cellular and Molecular Biology.*, (122).

Cooper, S., & Helmstetter, C. E. (1968). Chromosome replication and the division cycle of Escherichia coli B/r. *Journal of molecular biology*, *31*(3), 519–40.

Klumpp, S., Zhang, Z., & Hwa, T. (2009). Growth Rate-Dependent Global Effects on Gene Expression in Bacteria. *Cell, Volume 139, Issue 7, 1366-1375, 24 December 2009*, 1366–1375.

Kochanowski, K., Volkmer, B., Gerosa, L., R Haverkorn van Rijsewijk, B., Schmidt, A., & Heinemann, M. (2013). Functioning of a metabolic flux sensor in Escherichia coli. *Proceedings of the National Academy of Sciences of the United States of America*, *110*(3), 1130–5. doi:10.1073/pnas.1202582110

Kubitschek, H. (1974). Constancy of the ratio of DNA to cell volume in steady-state cultures of Escherichia coli B-r. *Biophysical Journal*, *14*(2), 119–123. doi:10.1016/S0006-3495(74)70003-0

Liang, S., Bipatnath, M., Xu, Y., Chen, S., Dennis, P. P., Ehrenberg, M., & Bremer, H. (1999). Activities of constitutive promoters in Escherichia coli. *Journal of molecular biology*, *292*(1), 19–37. doi:10.1006/jmbi.1999.3056

Zaslaver, A., Bren, A., Ronen, M., Itzkovitz, S., Kikoin, I., Shavit, S., Liebermeister, W., et al. (2006). A comprehensive library of fluorescent transcriptional reporters for Escherichia coli. *Nature Methods*, *3*(8), 623–628. doi:10.1038/NMETH895

Zaslaver, A., Mayo, A. E., Rosenberg, R., Bashkin, P., Sberro, H., Tsalyuk, M., Surette, M. G., et al. (2004). Just-in-time transcription program in metabolic pathways. *Nature genetics*, *36*(5), 486–91. doi:10.1038/ng1348